16

Real-Time Control System for a Two-Wheeled Inverted Pendulum Mobile Robot

Nawawi, Ahmad and Osman
Universiti Teknologi Malaysia
Malaysia

1. Introduction

The research on two-wheeled inverted pendulum (T-WIP) mobile robots or commonly known as balancing robots have gained momentum over the last decade in a number of robotic laboratories around the world (Solerno & Angeles, 2003;Grasser et al., 2002; Solerno & Angeles, 2007;Koyanagi, Lida & Yuta, 1992;Ha & Yuta, 1996; Kim, Kim & Kwak, 2003). This chapter describes the hardware design of such a robot. The objective of the design is to develop a T-WIP mobile robot as well as MATLAB™ interfacing configuration to be used as flexible platform which comprises of embedded unstable linear plant intended for research and teaching purposes. Issues such as selection of actuators and sensors, signal processing units, MATLAB™ Real Time Workshop coding, modeling and control scheme is addressed and discussed. The system is then tested using a well-known state feedback controller to verify its functionality.

2. Hardware development

Figure 1 show the CAD illustration of the T-WIP mobile robot towards the real hardware. The robot is equipped with two servo drives for actuation, a Gyroscope for measuring angle and angular velocity of pendulum body, and encoders for measuring the position of the wheels. Signal processing and control algorithm are distributed among three microprocessors. Two of them are used for servo drives while other one is used for stabilizing control.

Although this kind of layout enables hierarchical control design, it also complicates implementation, since processor communication must also be considered (Kim & Kwak, 2003). The T-WIP mobile robot is composed of a chassis carrying a DC motor coupled to a planetary gearbox for each wheel, the DSP board used to implement the controller, the power amplifiers for the motors, the necessary sensors to measure the vehicle's states. The battery is bolted inside the body casing and it significantly represents 30% of the total robot mass. The wheels of the vehicle are directly coupled to the output shaft of the gearboxes. The robot is control by applying a torque C_R and C_L to the right and left wheels respectively. Figure 2 illustrates the block diagram of the control architecture of the system.

The controller is implemented on an Embedded DSP board by Googol Technologies LTD (2007). It is a standalone motion controller based on combination of embedded PC104 main board of X86, motion control board, terminal board in one structure, and thus has the advantages of smaller dimension, less wiring, real time capability and higher reliability. It is easy to upgrade, install and maintain, and thus increase the reliability of the robot to operate under adverse industrial environments, such as humid, dust, and vibration.

Conventional inclinometers, or analog tilt sensors, typically exhibit slow response and cannot be used to track dynamic angular motion (Tsuchiya, Urakubo & Tsujita, 1999; Matsumoto, Kajita & Tani, 1993). On the other hand, angular rate sensors can be used to measure fast rotations, but they suffer from significant drift and error accumulation over time. Inertial measurement units (IMU's) can be used to overcome these limitations, but these are relatively large and expensive. As such, the FAS-G sensor from MicroStrain is used as the gyro sensor (FAS-G Microstrain, 2006).

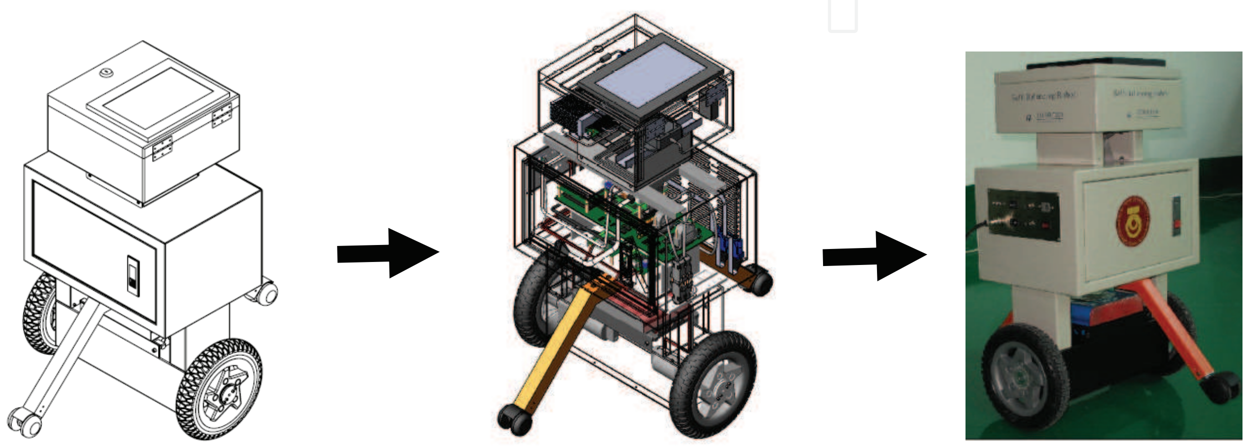

Fig. 1. CAD Illustration of T-WIP Mobile Robot towards Real Hardware

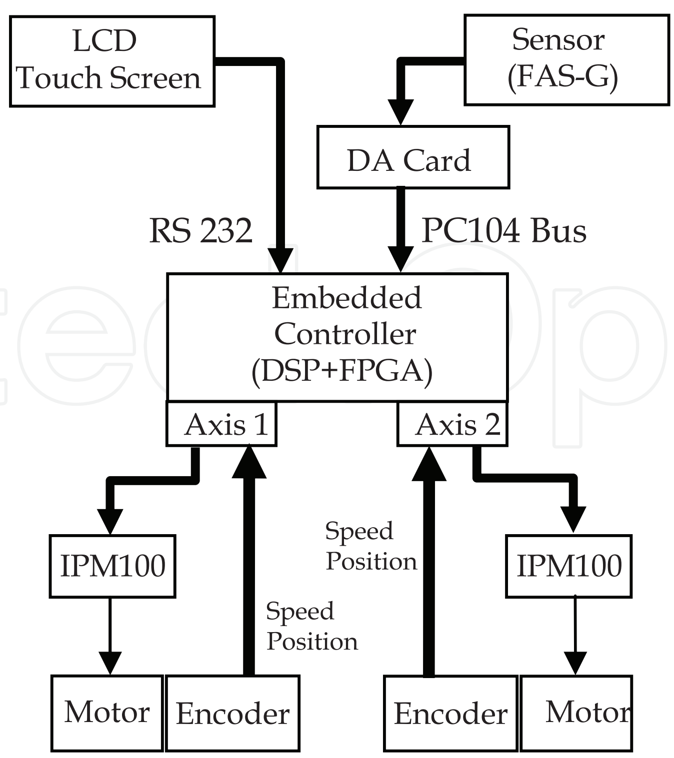

Fig. 2. Control Architecture

Employing micro-electromechanical (MEM) sensors, FAS-G consists of a combination of two low pass filtered accelerometers and one piezo-ceramic gyro. The angular rate signal is integrated internally over time and compared to the accelerometer signal to eliminate drift. The gyro output signal is an analog voltage between 0 and 5 volts corresponding to the angle of tilt. This signal is read from the Data Acquisition Card and the result is passed to PC by PC104 data bus. It was calculated that one ADC count corresponds to an incremental tilt of 0.08789º. A secondary angular rate signal is also generated by means of software computation. Figure 3 show angle of rotation for a two-wheeled inverted pendulum mobile robot in two-dimensional plane. Both geared servo motor needs to generate a very high torque. To achieve this, the IPM100 is used as the motor driver. It is basically a 36V, 3A fully digital intelligent servo drive based on the DSP controller technology. It is also embedded with the high level Technosoft Motion Language (TML) and therefore offers a flexible, compact and easy to implement solution for single or multi-axis applications with brushless and DC motors.

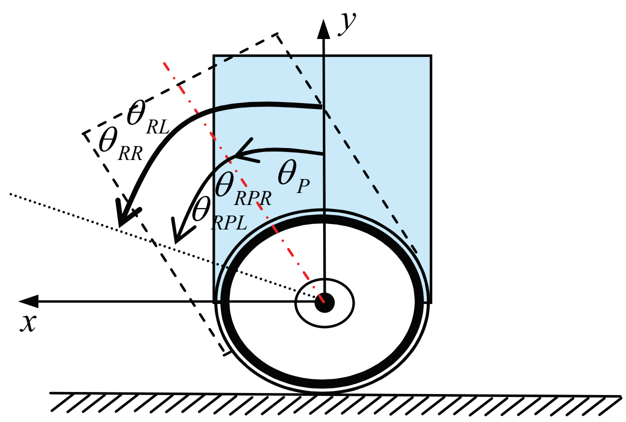

Fig. 3. Angle of Rotational

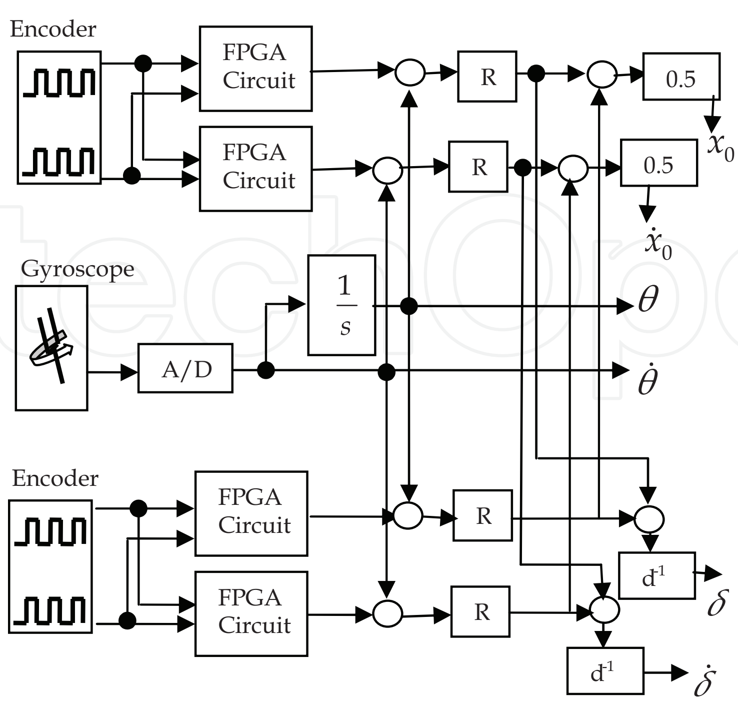

Fig. 4. Interfacing between sensor signals and the Embedded DSP board (Grasser et al. 2002)

Straight line position and speed as well as yaw angle and rate of change can be determined from the angle rotation of the two wheels (θ_{RR} and θ_{RR}) with respect to the gravity. The relation of these angles with pitch angle, θ_P and the body angle, θ_{RPL} and θ_{RPR} can be referred in Fig.3. To provide information about T-WIP states for control purposes, two incremental encoders and a rate gyroscope are interfaced together as shown in Fig.4. All the interfacing is based on control structure of embedded system as seen in this figure. The embedded controller has task to monitor all feedback coming from incremental encoder. Then process the feedback to make sure T-WIP is balance at it equilibrium point. The command to embedded controller is given by IPC using C language interfacing in the Real Time Workshop of MATLAB. The IPC is running online or at the same time with system to show the real time result according to the output response needed.

3. Mathematical modeling

The dynamic performance of a balancing robot depends on the efficiency of the control algorithms and the dynamic model of the system (Shim, Kim & Koh, 1995;Au, Xu & Yu, 2001). By adopting the coordinate system shown in Fig.5 using Newtonian mechanics, it can be shown that the dynamics of the T-WIP mobile robot under consideration is governed by the following motion equations (1)-(15). The coordinate system for the robot is depicted in Fig.5.

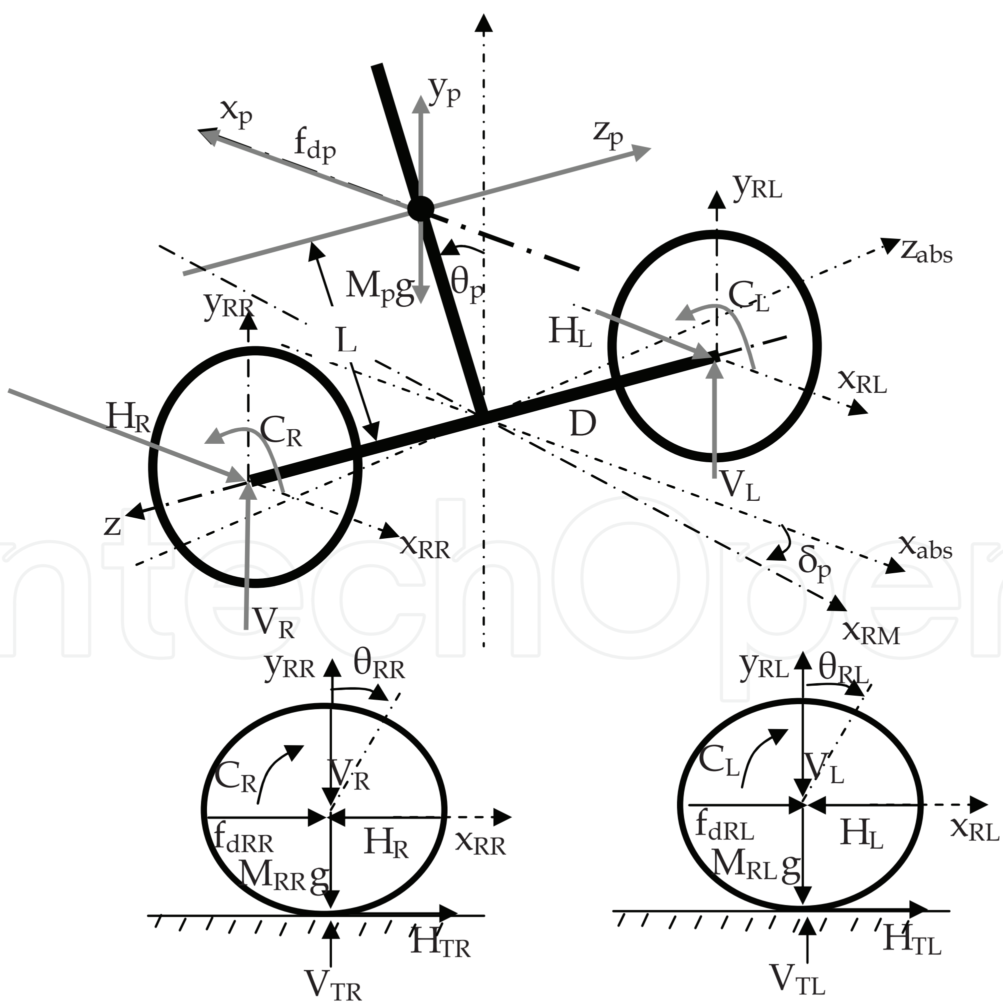

Fig. 5. Coordinate system of the T-WIP

For left hand wheel (analogous for right hand wheel):

$$\ddot{x}_{RL}M_r = H_{TL} - H_L + (f_{dRL} + f_{dRR}) \tag{1}$$

$$\ddot{y}_{RL}M_r = V_{TL} - V_L - M_r g \tag{2}$$

$$\ddot{\theta}_{RL}J_{RL} = C_L - H_{TL}R \tag{3}$$

$$\dot{x}_{RL} = R\dot{\theta}_{RL} \tag{4}$$

$$\dot{y}_p = -\dot{\theta}_p L \sin\dot{\theta}_p \tag{5}$$

$$\dot{x}_p = \dot{\theta}_p L \cos\theta_p + \frac{\dot{x}_{RL} + \dot{x}_{RR}}{2} \tag{6}$$

$$\dot{\delta} = \frac{\dot{x}_{RL} - \dot{x}_{RR}}{2f} \tag{7}$$

For the chassis, the equations:

$$\ddot{x}_p M_p = (H_R + H_L) + f_{dP} \tag{8}$$

$$\ddot{y}_p M_p = V_R + V_L - M_p g + F_{C\theta} \tag{9}$$

$$\ddot{\theta}_p J_p = (V_R + V_L)L\sin\theta_p - (H_R + H_L)L\cos\theta_p - (C_L + C_R) \tag{10}$$

$$\ddot{\delta}J_\delta = (H_L - H_R)\frac{D}{2} \tag{11}$$

where H_{TL}, H_{TR}, H_L, H_R, V_{TL}, V_{TR}, V_L, V_R represent reaction forces between the different free bodies. The robot parameters are as tabulated in Table 6.1.
Equations (1)-(11) can be represented in the state-space form as:

$$\dot{x}(t) = f(x) + g(x)u \tag{12}$$

Where $x \in \mathbb{R}^n$, $u \in \mathbb{R}^m$ are respectively the state and the control. $f(x)$ is nonlinear dynamic function matrix and $g(x)$ is nonlinear input function matrix. The state, x of the system is defined as:

$$x = [x_r, \dot{x}_r, \theta_p, \dot{\theta}_p, \delta, \dot{\delta}]' \tag{13}$$

Modifying the equations above and then linearizing the result around the operating point (θ_p=0, x_r=0, δ=0) and de-coupling, the system's state space equations can be written in matrix form as:

$$\begin{bmatrix} \dot{x}_r \\ \ddot{x}_r \\ \dot{\theta}_p \\ \ddot{\theta}_p \end{bmatrix} = \begin{bmatrix} 0 & 1 & 0 & 0 \\ 0 & 0 & A_{23} & 0 \\ 0 & 0 & 0 & 1 \\ 0 & 0 & A_{43} & 0 \end{bmatrix} \begin{bmatrix} x_r \\ \dot{x}_r \\ \theta_p \\ \dot{\theta}_p \end{bmatrix} + \begin{bmatrix} 0 \\ B_2 \\ 0 \\ B_4 \end{bmatrix} [C_L + C_R] \tag{14}$$

$$\begin{bmatrix} \dot{\delta} \\ \ddot{\delta} \end{bmatrix} = \begin{bmatrix} 0 & 1 \\ 0 & 0 \end{bmatrix} \begin{bmatrix} \delta \\ \dot{\delta} \end{bmatrix} + \begin{bmatrix} 0 \\ B_6 \end{bmatrix} [C_L - C_R] \tag{15}$$

where

$$A_{23} = g(1 - \frac{4}{3} L \frac{M_p}{X})$$

$$A_{43} = \frac{gM_p}{X}$$

$$B_2 = (\frac{4LY}{3X} - \frac{1}{M_p L})$$

$$B_4 = -\frac{Y}{X}$$

$$B_6 = \frac{6}{(9M_r + M_p)RD}$$

and,

$$X = \frac{1}{3} \frac{M_p (M_p + 6M_r) L}{M_p + \frac{3}{2} M_r}, Y = \frac{M_p}{(M_p + \frac{3}{2} M_r) R} + \frac{1}{L}$$

For simplicity, the details of equation (14) and (15) are not shown here and can be found elsewhere (Felix et al., 2002;Nawawi, Ahmad & Osman, 2007). The T-WIP balancing model, namely equation (14) will be used through out this work.

4. Controller design

System performance (i.e. reaction to disturbance forces, tracking of driver input, etc.) is driven by the pole placement controller. In order to test the T-WIP performance, pole-placement controllers with different poles has been applied. For a chosen pole placement, the controller's gains were calculated and implemented on the embedded board. T-WIP was then tested with the configuration and the response is then recorded by the control system. One of the tests conducted consist of an impulse disturbance force applied to a position above the center of gravity. The energy transmitted with a falling weight amounted to about 1.2 J (Baloh & Parent, 2003).

Issues like damping ratio and settling time could be clearly identified on the recorded responses and permitted an efficient fine-tuning of the system. Figure 6 shows the system's response to the above mentioned test with the initial pole placement chosen at pole [-1.5,-1.5,-0.5-3i,-0.5+3i]. Note the pronounced oscillation of the system which indicates too weak damping. Increasing the damping ratio when change the pole to [-1.5-i,-1.5+i,-3.5-5i,-3.5+5i] give the result as shown in Fig.7. It can be seen that the response improves significantly.

Symbol	Parameter	Value/ [Unit]
x_r	Straight line position	[m]
θ_p	Pitch angle	[rad]
δ	Yaw angle	[rad]
J_{RL}, J_{RR}	Moment of inertia of the rotating masses with respect to the z axis	[kgm²]
M_r	Mass of rotating masses connected to the left and right wheel . $M_{RL} = M_{RR} = M_r$	0.420 [kg]
J_p	Moment of inertia of the chassis with respect to z axis	0.28 [kgm²]
J_δ	Moment of inertia of the chassis with respect to the y axis	1.12[kgm²]
M_p	Mass of Body	15.0 [kg]
R	Radius of wheel	0.106[m]
L	Distance between the z axis and the center of gravity of vehicle	0.4 [m]
D	Lateral distance between the contact patches of the wheels.	0.4[m]
y_r	Shift position of the wheel with respect to the y axis.	
x_p	Shift position of the chassis with respect to the x axis.	
g	Gravity constant	9.8 [ms⁻²]
C_L , C_R	Input torque for right and left wheels accordingly	

Table 1. Parameters of T-WIP

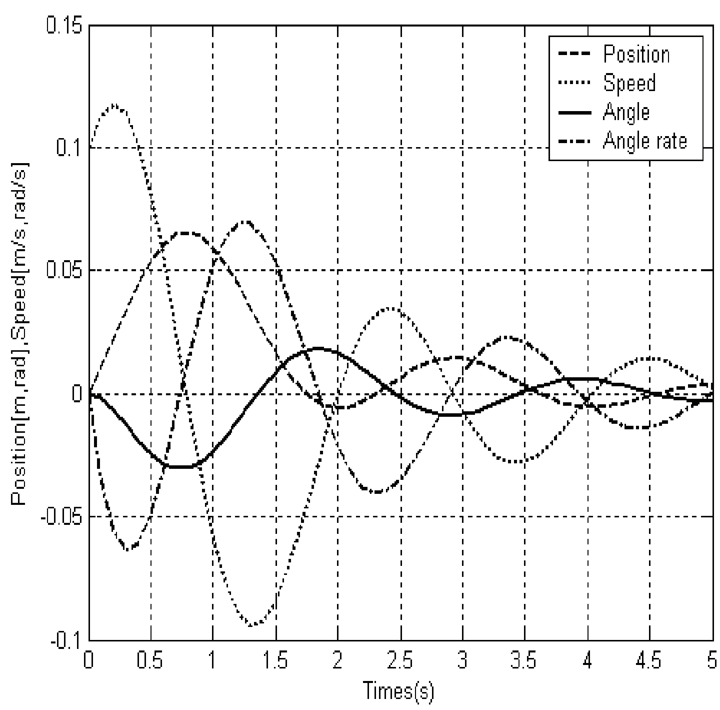

Fig. 6. Initial pole placement of the “pendulum” system and associated response to an impulse disturbance force

Now it has a harmonious catching of the disturbance force. When the force hit T-WIP, it causes the pendulum to fall forwards (θ_p<0). The control system accelerates the wheels in a positive direction to catch this fall and ultimately make the pendulum fall in the other direction. A negative torque is then applied, moving the vehicle back to its original position and getting the pendulum back in an upright position. The controller task is to make sure that:

$$\theta_p \in A_s = \left\{ \left| \theta_p \right| < \theta_m < \pi / 2 \right\} \text{, for a given } \theta_m > 0 \tag{16}$$

Equation (16) is representing physically problem of T-WIP, because by using these reference commands, one can safely follow a motion plan (Pathak & Agrawal, 2006). θ_m is maximum pitch angle setting for safety purpose. The pitch angle θ_p can be used as a gas pedal for vehicle and role it to accelerate and decelerate until the specified speed is attained.

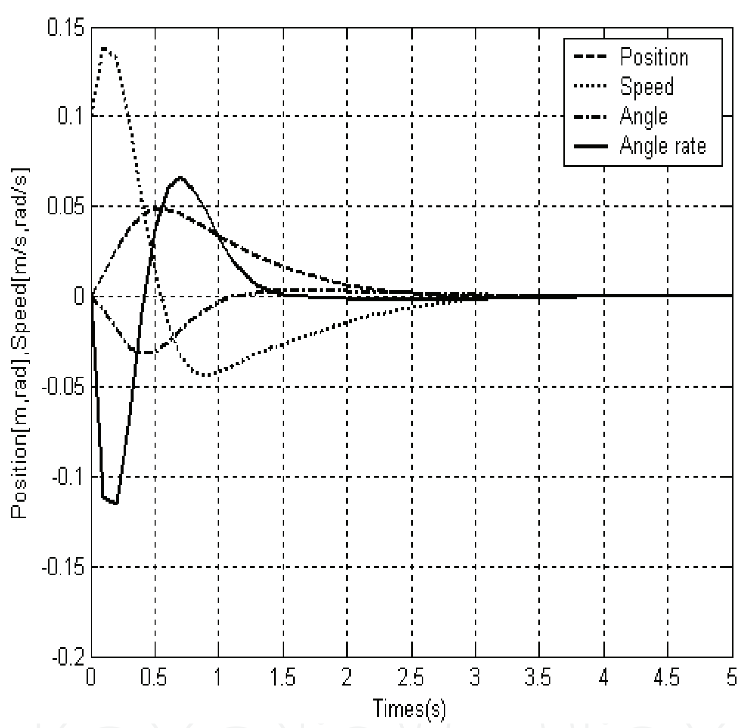

Fig. 7. Improved pole placement of the "pendulum" system and associated response to an impulse disturbance force.

Another issue that has been addressed during testing is drivability. In order to successfully improve drivability, it was characterized based on two criteria. First criteria are readouts of the system's reaction to a ramp shaped speed input and second criteria are the way different drivers felt about T-WIP handling. Combining the driver's feelings with the readouts of system behavior allowed further improvement of T-WIP control system. Figure 8 shows the system's response to a velocity ramp input with the final pole placement chosen. Note that the maximum acceleration possible is lower than the maximum deceleration. Due to the motor's speed-current characteristics, a high torque cannot be obtained when operating at high speeds (Matsumoto, Kajita & Tani, 1991). However, this is exactly what is necessary to get the vehicle back into an upright position at the end of the acceleration phase.

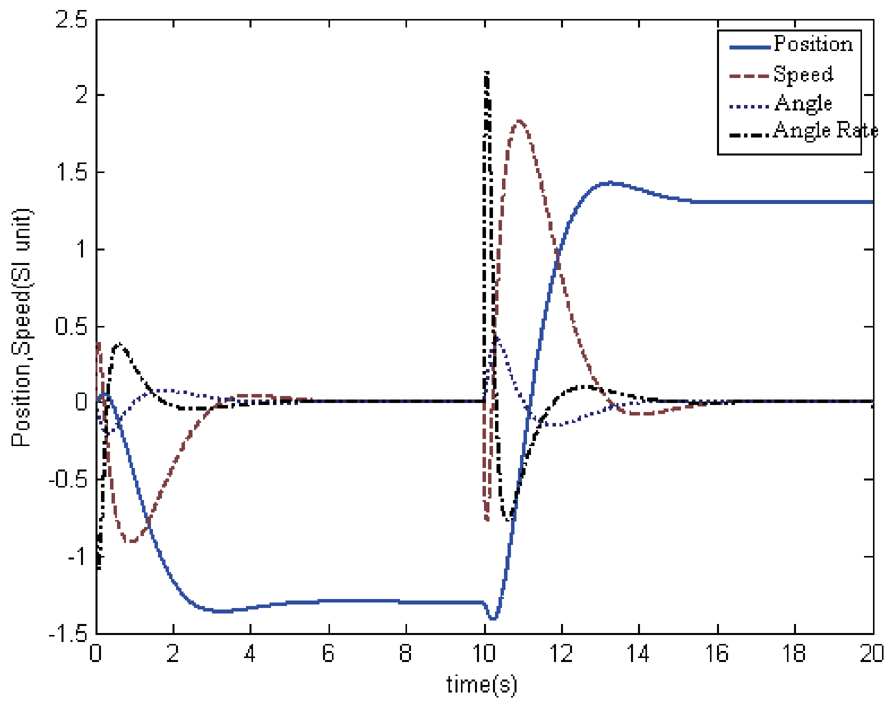

Fig. 8. Reaction to a ramp shaped speed input

Deceleration demands maximum torque at low speeds so a steeper ramp is therefore possible (Deniskina, Levi & Gurfinkel, 2001). Increasing performance with the pole placement chosen can be achieved by moving the poles further to the left, thus making the system faster. Backlash as well the maximum torque that can be transmitted to the ground (grip) prevent tuners from moving the poles past a certain limit. The used of an adaptive pole placement and nonlinear controller (depending on the system's state) would enable further improvements to the system.

5. Matlab™ interfacing design

The embedded control system in this work is design based on real-time workshop of MATLAB™. Hence it makes the interfacing protocol between embedded controller card and MATLAB™ is the most pivotal. T-WIP real-time balancing will be fully carried out in the Real Time Workshop of MATLAB™. Therefore it has an advantages of be intellectualized to observe the real-time results and performance of controller when be integrated with actuator. Furthermore, the controller can be redesigned expediently and repetitiously until users get a satisfactory result.

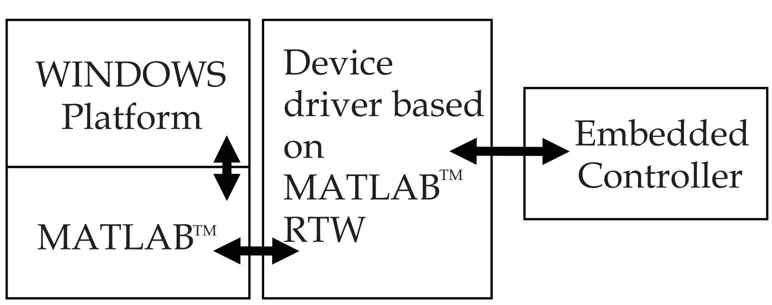

Fig. 9. MATLAB™ RTW Kernel

In the RTW (Real Time Workshop) of MATLAB™, the special real-time kernel model replaces message processing via windows as shown in Fig. 9. Hence the capability of real-time mode to gets better response is good enough.

RTW builds applications from Simulink diagrams for prototyping, testing, and deploying real-time systems on a variety of target computing platforms. Users of Real-Time Workshop can direct it to generate source code that accommodates the compilers, input and output devices, memory models, communication modes, and other characteristics that their applications may require. First step of configuration setup is to install MATLAB™ with Real-Time Windows Target and Visual C/C++ software. Then by using some command in Matlab, the Real-Time Windows Target kernel is activated together menu to select C compiler in MATLAB™.

A sampling demo of the sensor will be presented based on MATLAB™ RTW. In way to design an S-function block written in C Language, in which an S-function parameter for index of ad channels and an output should be defined. The fractional source code of GetAD.c is as follows:

```
#define S_FUNCTION_NAME   GetAD
#define NUM_PARAMS              (1)
#define AD_CHANNEL  _PARAM  (ssGetSFcnParam(S,0))
#define AD_CHANNEL (real_T)mxGetPr(AD_CHANNEL_PARAM)[0])
```

After coding for GetAD.c, by using a command line in MATLAB with no errors occur, the GetAD S-function then finished generating. Then the block parameter for ad channel is configured to channel 1. Secondly another system target file GetAD.tlc need to be design which is will be saved in the same directory with GetAD.c. The main source code flow chart of GetAD.tlc is as shown in Fig. 10.

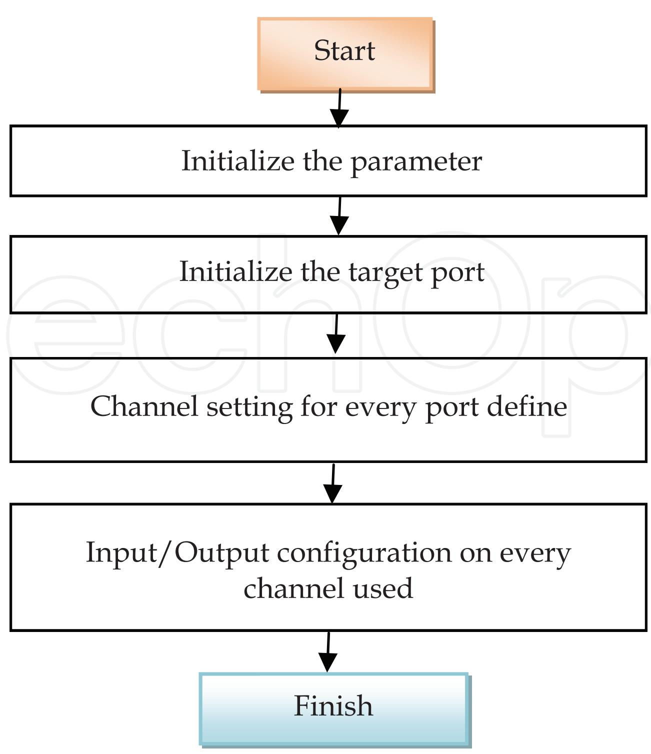

Fig. 10. Coding flowchart for GETAD.tcl

For the reference purpose, the command "_outp" and "_inp" in the target file GetAD.tlc is used for sending and receiving data between embedded controller and MATLAB™. The comand ctrl_byte=oxff , is used in GetAD.tlc file to make sure the DA card will stop find online data on the PC104 bus. GetAD.tlc then compiled and be confirmed there is no error occurs.

In simulation parameter properties of GetAD.c, category need to build as Target configuration with system target file of rtwin.tlc. This configuration is used as setting for Real-time workshop in Matlab. Then the solver options and fixed step size configuration is set with sampling time 5ms.

The file is compiled after selecting "External" mode. The output of the sensor signal can be shown in Fig. 11. The same method is using to design other S-functions models. Finally, an interface for T-WIP in the RTW of MATLAB™ is extracted. Now T-WIP test bed can be used for any type of controller as long as the structure of system remains the same. The structure of system is shown in Fig. 12.

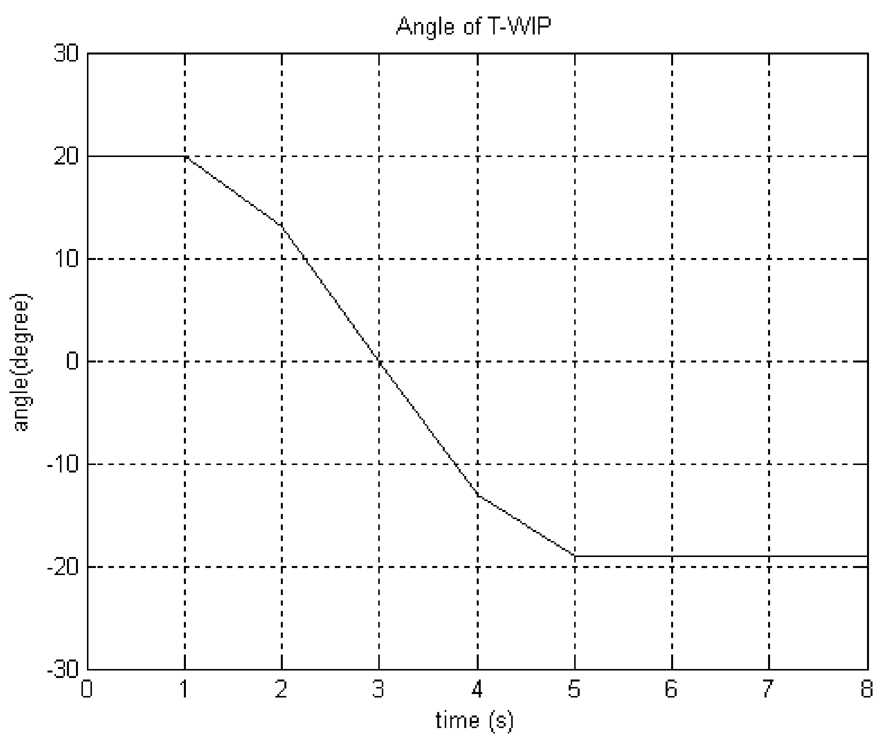

Fig. 11. Angle for sampling gyro sensor

It does consist of three main block which is Input block, controller block and Real Plant block. The input reference for speed and orientation can be replaced by desired input function while the real plant block is the actual input function is used. The real plant block is the actual plant represents the hardware of T-WIP which contains of all sensors interfacing.

6. Experimental result

In order to verify the developed T-WIP hardware system, the pole-placement algorithm as designed in previous section implemented as the controller. Figure 13 shows that the responses of the system closely match the simulation result in Figure 7 which demonstrates the complete T-WIP system is functioning well in close-loop system.

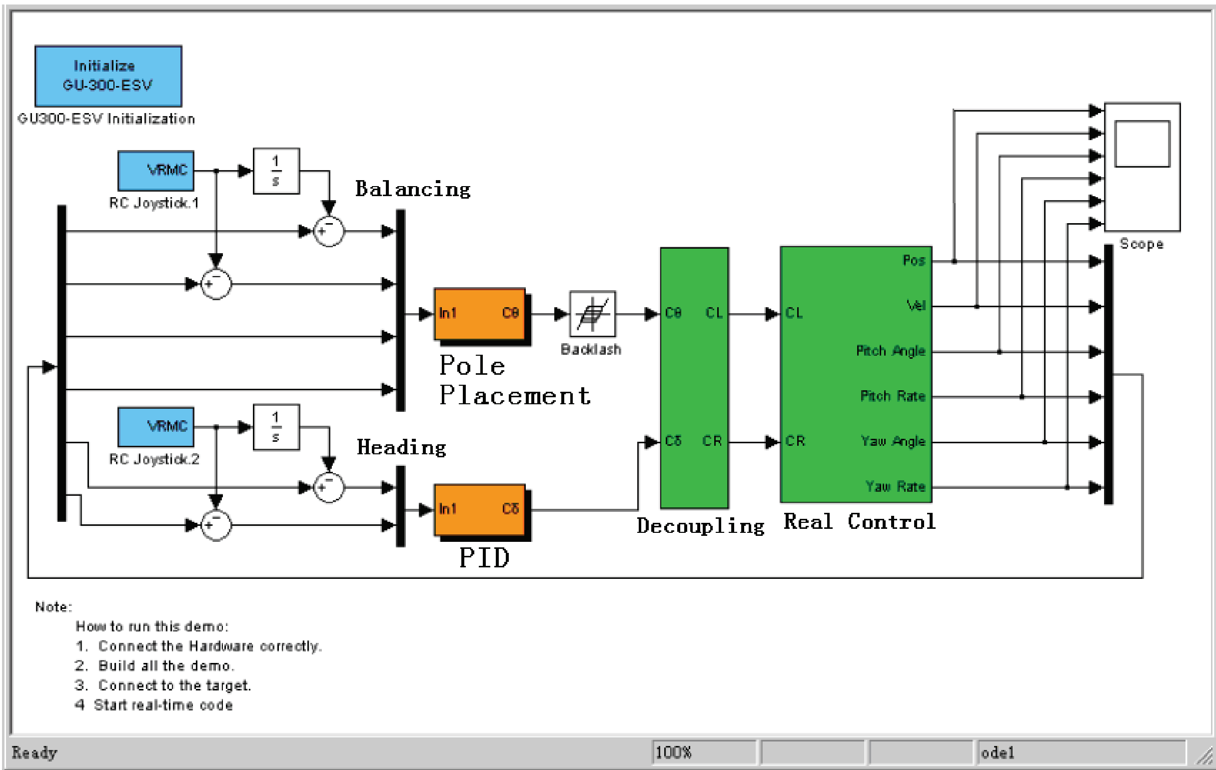

Fig. 12. Real-time control interface using poleplacement controller for T-WIP.

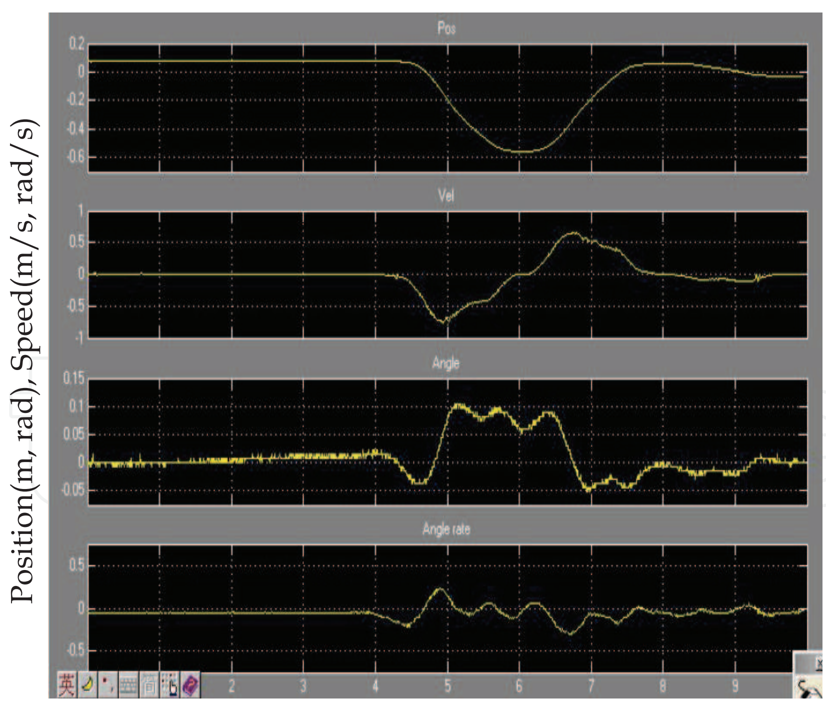

Fig. 13. Real-time control result of T-WIP output response using pole placement controller

From the Fig. 13, it can be shown that the output response for position, velocity, inclination angle and angular velocity of inclination is following the shape of simulation result. The steady state error of position and velocity is approximately zero. It also shows that the values of steady state error are about zero of the inclination angle and its velocity.

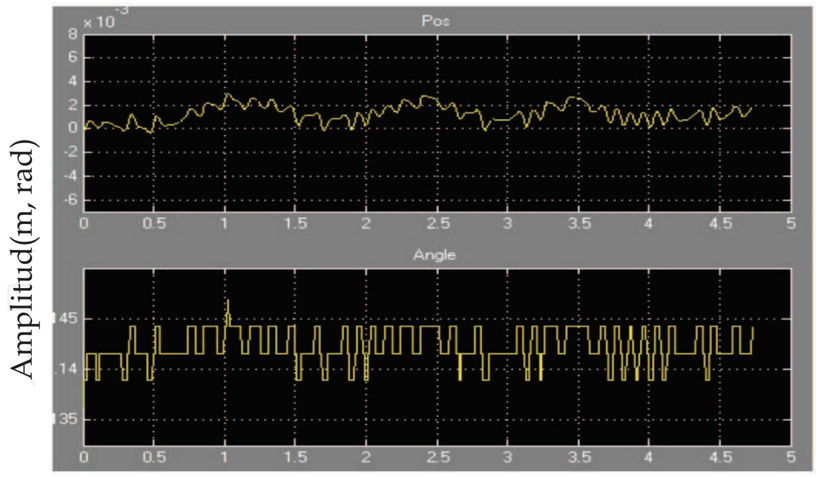

Fig. 14. Real-time control results of vibration scale for T-WIP at equilibrium

The pole placement controller seems to be capable in term of steady state error and settling time. After zooming in certain area on Fig. 13, it can be seen on result in Fig. 14, it shown that the system is in equilibrium within small range of vibration. The chassis range of vibration is about $4x10^{-3}$m and the trunk vibration range is about 0.05rad.

7. Conclusion

In this chapter, the development of a T-WIP mobile robot system is presented. The issues of dynamical modeling, selection of actuators and sensors, MATLAB™ based interfacing and configuration of the embedded controller, as well as the implementation of pole placement control strategy has been addressed. The embedded control system using real-time workshop of MATLAB is confirm working well and all sensors give a good feedback signal based on the response getting from the experimental work. The results from this work show that the proposed embedded design architecture based on MATLAB™ is capable of delivering the desired outcome and the T-WIP test rig is ready to be tested with a various type of controllers.

8. References

Au, S. K. W., Xu, Y. and Yu, W. W. K. (2001). Control of Till Up Motion of a Single Wheel Robot via Model Based and Human Based Controller. *Mechatronics.* 11, 451-473.

Baloh, M. and Parent, M. (2003). Modeling and Model Verification of an Intelligent Self-balancing Two Wheeled Vehicle for an Autonomous Urban Transportation System. *In Proceedings of Conference on Computational Intelligence Robotic and Autonomous Systems*. 15 Disember. Singapore: 1-7.

Deniskina, I. V., Levi, K. Y. S. and Gurfinkel, V. S. (2001). Relative Roles of the Ankle and Hip Muscles in Human Postural Control in the Frontal Plane Surfing Standing. *Journal of Intelligent Robot System.* 27(3), 317-321.

FAS-G Gyroscope Manual by Microstrian, available:http://www.microstrain.com/fas-g.asp

Googol Technology (HK). *All in one embedded motion controller specification.* [Online]. Available: http://www.googoltech.com

Grasser, F., D'Arrigo, A., Colombi, S. and Rufer, A. (2002). Joe: A Mobile Inverted Pendulum. *IEEE Transaction Electronics*. 49(1), 107-114.

Ha, Y. S. and Yuta, S. (1996). Trajectory Tracking Control for Navigation of The Inverse Pendulum Type Self-contained Mobile Robot. *Robotic and Autonomous System.* 17, 65-80.

Kim, Y.H., Kim, S.H., and Kwak, Y.K. (2003). Dynamic Analysis of a NonholonomicTwo-wheeled Inverted Pendulum Robot. *In Proceedings of 8th International Symposium on Artificial Life and Robotics*. 24-26 January. Beppu, Oita, Japan: 415-418.

Koyanagi, E., Lida, S. and Yuta, S. (1992). A Wheeled Inverse Pendulum Type Self-contained Mobile Robot and its Two-dimensional Trajectory Control. *In Proceedings of 2nd International Sysmposium on Measurement and Control in Robotics*. November. Tsukaba, Japan: 891-898.

Matsumoto, O., Kajita, S. and Tani, K. (1991). Attitude Estimation of the Wheeled Inverted Pendulum Using Adaptive Observer, *In Proceedings of 9th Academic Conference of the Robotics Society of Japan*. Japan: 909-910.

Matsumoto, O., Kajita, S. and Tani, K. (1993). Estimation and Control of the Attitude of a Dynamic Mobile Robot using Internal Sensors. *Advance Robotic.* 7(2), 159-178.

Nawawi, S. W., Ahmad, M. N. and Osman, J. H. S. (2007). Development of Two-wheeled Inverted Pendulum Mobile Robot. *In Proceedings Student Conference on Research and Development*. December. Kuala Lumpur, Malaysia: 153-158.

Pathak, K., Franch, J. and Agrawal, S. K. (2005). Velocity and Position Control of a Wheeled Inverted Pendulum by Partial Feedback Linearization. *IEEE Transactions on Robotics.* 21(3), 505-513.

Pathak, K. and Agrawal, S. K. (2006). Band-limited Trajectory Planning and Tracking for Certain Dynamically Stabilized Mobile Systems. *Journal of Dynamic Systems, Measurement and Control, Transaction of the ASME*. 128(1), 104-111.

Salerno, A. and Angeles J. (2003). Nonlinear Conrollability of Quasiholonomic Mobile Robot. In *Proceedings of IEEE ICRA*, 3379-3384, Taiwan.

Shim, H. S., Kim, J. H. and Koh, K. (1995). Variable Structure Control of Nonholonomic Wheeled Mobile Robot. *In Proceedings of IEEE International Conference on Robotics and Automation*. 21-27 May. Nagoya, Aichi, Japan: 1694-1699.

Solerno, A. and Angeles, J. (2007). A New Family of Two Wheeled Mobile Robot: Modeling and Controllability. *IEEE Transaction of Robotics.* 23(1), 169-173.

Tsuchiya, K., Urakubo, T. and Tsujita, K. (1999). A Motion Control of a Two-Wheeled Mobile Robot. *In Proceeding of IEEE International Conference on System, Man and Cybernetics*. October. Tokyo, Japan: 690-696.

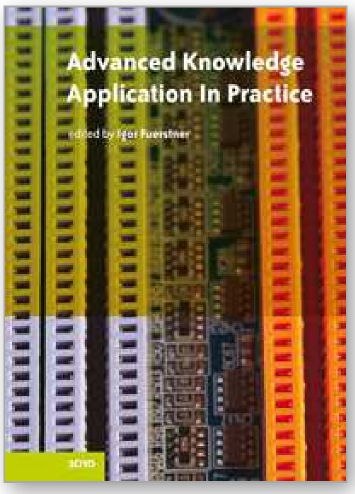

Advanced Knowledge Application in Practice

Edited by Igor Fuerstner

ISBN 978-953-307-141-1

Hard cover, 378 pages

Publisher Sciyo

Published online 02, November, 2010

Published in print edition November, 2010

The integration and interdependency of the world economy leads towards the creation of a global market that offers more opportunities, but is also more complex and competitive than ever before. Therefore widespread research activity is necessary if one is to remain successful on the market. This book is the result of research and development activities from a number of researchers worldwide, covering concrete fields of research.